

Accepted Manuscript

Urea cycle dysregulation in non-alcoholic fatty liver disease

Francesco De Chiara, Sara Heebøll, Giusi Marrone, Carmina Montoliu, Stephen Hamilton-Dutoit, Antonio Ferrandez, Fausto Andreola, Krista Rombouts, Henning Grønbaek, Vicente Felipo, Jordi Gracia-Sancho, Rajeshwar P Mookerjee, Hendrik Vilstrup, Rajiv Jalan, Karen Louise Thomsen

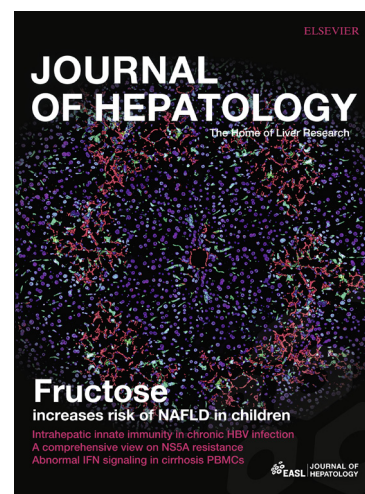
PII: S0168-8278(18)32176-7
DOI: <https://doi.org/10.1016/j.jhep.2018.06.023>
Reference: JHEPAT 7024

To appear in: *Journal of Hepatology*

Received Date: 20 December 2017
Revised Date: 22 June 2018
Accepted Date: 24 June 2018

Please cite this article as: De Chiara, F., Heebøll, S., Marrone, G., Montoliu, C., Hamilton-Dutoit, S., Ferrandez, A., Andreola, F., Rombouts, K., Grønbaek, H., Felipo, V., Gracia-Sancho, J., Mookerjee, R.P., Vilstrup, H., Jalan, R., Thomsen, K.L., Urea cycle dysregulation in non-alcoholic fatty liver disease, *Journal of Hepatology* (2018), doi: <https://doi.org/10.1016/j.jhep.2018.06.023>

This is a PDF file of an unedited manuscript that has been accepted for publication. As a service to our customers we are providing this early version of the manuscript. The manuscript will undergo copyediting, typesetting, and review of the resulting proof before it is published in its final form. Please note that during the production process errors may be discovered which could affect the content, and all legal disclaimers that apply to the journal pertain.



Urea cycle dysregulation in non-alcoholic fatty liver disease

Francesco De Chiara¹, Sara Heebøll², Giusi Marrone¹, Carmina Montoliu³,
Stephen Hamilton-Dutoit⁴, Antonio Ferrandez⁵, Fausto Andreola¹,
Krista Rombouts¹, Henning Grønbaek², Vicente Felipo⁶, Jordi Gracia-Sancho⁷, Rajeshwar P
Mookerjee¹, Hendrik Vilstrup², *Rajiv Jalan¹, *Karen Louise Thomsen^{1,2}

*Joint senior authors

¹ UCL Institute of Liver and Digestive Health, University College London, United Kingdom

² Department of Hepatology & Gastroenterology, Aarhus University Hospital, Denmark

³ Fundación Investigación Hospital Clínico de Valencia. Instituto de
Investigación Sanitaria-INCLIVA, Valencia, Spain

⁴ Institute of Pathology, Aarhus University Hospital, Denmark

⁵ Anatomía Patológica Hospital Clínico Universitario, Valencia, Spain

⁶ Laboratory of Neurobiology, Centro Investigación Príncipe Felipe de
Valencia, Spain

⁷ Liver Vascular Biology Research Group, IDIBAPS Biomedical Research Institute & CIBEREHD, Barcelona,
Spain

Correspondence:

Professor Rajiv Jalan
UCL Institute of Liver and Digestive Health
University College London
Royal Free Campus
Rowland Hill Street
London NW32PF
United Kingdom
Phone (direct): +44 2074332795
E-mail: r.jalan@ucl.ac.uk

Dr Karen Louise Thomsen
Department of Hepatology & Gastroenterology,
Aarhus University Hospital,
Palle Juul-Jensens Boulevard
8200 Aarhus N
Denmark
Phone (direct): +45 78453811
E-mail: karethom@rm.dk

Number of figures and tables: 7 figures / 1 table

Conflict of interest

Rajiv Jalan has on-going research collaborations with Yaqrit and Takeda. He is also inventor of a drug, L-ornithine phenyl acetate (OCR-002), which UCL has licensed to Mallinckrodt Pharma. He is also the founder of UCL spin-out company Yaqrit Ltd. and Cyberliver Ltd. Henning Grønbæk has received research grants from the NOVO Nordisk Foundation, Abbvie and Intercept. All other authors have nothing to disclose.

Financial support

This study was generously supported by grants from the Novo Nordisk foundation, the Danish Council for Independent Research and Ministerio de Ciencia e Innovación (SAF2014-51851-R to V.F., and FIS PI15/00035 ISCIII to C.M.).

Author contributions

FDC, HG, RJ and KLT conceived and designed the study. SH, CM, and KLT carried out the experiments. FDC, GM, SHD, AF, FA and JGS analysed the samples. FDC, FA, RJ and KLT analysed and interpreted the data. KLT and FDC drafted the manuscript. HV, RJ, KR and RM critically revised the manuscript for important intellectual content. All authors read and approved the final manuscript.

ABSTRACT

Background: In non-alcoholic steatohepatitis (NASH), function of urea cycle enzymes (UCEs) may be affected and result in hyperammonemia with risk of disease progression. We aimed to determine whether expression and function of UCEs are altered in a NASH animal model and in non-alcoholic fatty liver disease (NAFLD) patients and whether this is reversible.

Methods: Rats were fed a high-fat, high-cholesterol diet for 10 months to induce NASH and then changed to normal chow to recover. In humans, we obtained liver biopsies from 20 patients with steatosis and 15 NASH patients. Primary rat hepatocytes were isolated and cultured with free fatty acids. We measured the gene and protein expression, the activity of ornithine transcarbamylase (OTC) and ammonia concentrations. Moreover, we assessed the promoter methylation status of OTC and carbamoyl phosphate synthetase (CPS1) in rats, humans and in steatotic hepatocytes.

Results: In NASH animals, gene and protein expression of OTC and CPS1 and activity of OTC were reversibly reduced and hypermethylation of OTC promoter genes was observed. Also in NAFLD patients, OTC enzyme concentration and activity were reduced and ammonia concentrations were increased and more so in NASH. Furthermore, OTC and CPS1 promoter regions were hypermethylated. In primary hepatocytes induction of steatosis was associated with OTC promoter hypermethylation, reduction in the gene expression of OTC and CPS1 and an increase in ammonia concentration in the supernatant.

Conclusion: NASH is associated with a reduction in gene and protein expression, and activity of UCEs resulting in hyperammonemia, possibly through hypermethylation of UCE genes and impairment of urea synthesis. Our investigations describe for the first time a link

between NASH, function of UCEs and hyperammonemia providing a novel therapeutic target.

Word count: 275

Key words: ammonia, epigenetic modifications, non-alcoholic fatty liver disease, non-alcoholic steatohepatitis, urea synthesis.

Lay summary: In patients with fatty liver disease, the enzymes that convert nitrogen waste into urea may be affected leading to the accumulation of the toxic substance, ammonia. This accumulation of ammonia can lead to development of scar tissue and risk of progression of disease. In this study, we show that fat accumulation in the liver produces a reversible reduction in the function of these enzymes that are involved in detoxification of ammonia. These data provide potential new targets for therapy of fatty liver disease.

INTRODUCTION

Alarming increases in obesity and in rates of non-alcoholic fatty liver disease (NAFLD) in an ageing population, mean that liver disease is a great health concern over the next decade (1, 2). NAFLD is a spectrum of liver disease ranging from steatosis, through non-alcoholic steatohepatitis (NASH) to cirrhosis (3). Recently, NASH has been defined as a “multiple parallel hits” disease (4) that can progress to liver fibrosis, which is the principal factor contributing to NASH-associated morbidity and mortality (5, 6). The main cell type responsible for extracellular matrix deposition is the hepatic stellate cell (HSC), which undergo activation in conditions of frank hepatocellular injury, enabling them to participate in the wound healing process (7) and making them key in the development of fibrosis.

The urea cycle, located exclusively in the liver, has evolved in humans to remove ammonia. The enzymes involved in this process are carbamoylphosphate synthetase (CPS1), ornithine transcarbamylase (OTC), argininosuccinate synthetase (ASS), argininosuccinate lyase (ASL) and arginase (ARG), but only the first two are present in the mitochondria (8). In NASH, many lines of investigation indicate that mitochondria are dysfunctional (9). It is, therefore, possible that the resultant mitochondrial injury leads to a modification of OTC and CPS1 genes, reducing their expression and function, and resulting in hyperammonemia. Accordingly, we have previously shown in an experimental, diet-induced NASH model, that gene and protein expressions of OTC and CPS1 were reduced significantly, resulting in functional reduction in the *in vivo* capacity for ureagenesis (10). This impairs nitrogen homeostasis and results in hyperammonemia.

We have recently demonstrated that pathological ammonia concentrations produce changes in human HSC behaviour, including significant alterations in cellular morphology, reactive oxygen species production and further HSC activation (11). Removal of ammonia from the cell cultures restored HSC morphology and function towards normality indicating that the changes in the HSCs induced by ammonia are reversible (11). These *in vitro* data were substantiated in bile duct-ligated rats with advanced fibrosis and hyperammonemia where treatment with the ammonia lowering drug ornithine-phenylacetate significantly reduced plasma ammonia, markers of HSC activation and portal pressure indicating that targeting ammonia *in vivo* reduces HSC activation (11).

The aims of this study were to determine if reduced gene and protein expression, and function of urea cycle enzymes (UCEs) induced hyperammonemia in an animal model of NASH, and also to determine if this process was reversible by restoring the diet. To confirm the animal data, we determined plasma and liver ammonia, OTC gene and protein expression and activity in liver biopsies from NAFLD patients. To investigate the potential mechanism underlying these changes, the methylation status of UCEs' promoter regions were assessed both in rats and humans and *in vitro* studies in primary rat hepatocytes inducing steatosis were performed.

MATERIAL AND METHODS

Animal study

Female Wistar rats (body weight 200-220 g; Taconic M&B, Ejby, Denmark) were housed at $21\pm 2^{\circ}\text{C}$ with a 12-h artificial light cycle. Three animals were housed in each cage with free access to tap water. All animals were allowed to acclimatise on a standard diet for a week followed by randomization. Half of the rats were fed a standard diet (D12450J) and the other half a high-fat, high-cholesterol diet (HFHC) diet (D09052204) *ad libitum* (both from Research Diets, New Brunswick, NJ, USA). The standard diet was composed of the following energy sources: 67 g carbohydrates (70 kcal%), 4 g fat (10 kcal%), and 19 g protein (20 kcal%) per 100 g diet. The HFHC diet contained 19 g carbohydrates (15 kcal%), 39 g fat (65 kcal%), 2 g cholesterol, and 27 g protein (20 kcal%) per 100 g diet. The study was performed in accordance with local and national guidelines for animal welfare and approved by the institutional Animal Ethics Committee.

Design

Thirty animals were divided into five groups: two receiving standard diet and two HFHC diet for 10 and 12 months, respectively. The fifth group received HFHC diet for 10 months and was then changed back to normal diet for two months. After an overnight 12-h fast the animals were anaesthetised with a subcutaneous injection of fentanyl/fluanisone (Hypnorm®, Jansen Pharma, Birkerød, Denmark) at $0.5 \text{ mL} \times \text{kg}^{-1}$ and midazolam (Dormicum®, La Roche, Basel, Switzerland) at $2.5 \text{ mg} \times \text{kg}^{-1}$. All blood was collected for analyses. The liver and spleen were weighed and slices of liver tissue from the left lobe were secured, fixed overnight in 10% buffered formalin and embedded the next day in paraffin. Sections were stained with hematoxylin-eosin (H&E) and Sirius Red for

histological examination. Additionally, 200 mg of liver tissue was snap-frozen in liquid nitrogen, and stored at -80°C . The following variables were determined in plasma: bilirubin, alanine aminotransferase (ALT), albumin, glucose, total cholesterol and triglycerides concentrations. In liver tissue, we determined triglycerides, mRNA levels of the UCEs CPS1, OTC, ASS, ASL and ARG; protein expression of CPS1 and OTC; enzyme activity of OTC, global methylation and methylation of the promoter of the OTC gene.

Liver histology

All histology specimens were reviewed by an experienced liver histopathologist (SHD) blinded to the clinical and laboratory data. Histological parameters were scored according to standard criteria (12).

Blood analyses

Plasma ALT, bilirubin, albumin, glucose, total cholesterol and triglycerides were determined by routine analytical methods. All of the assays used in this study had been validated for use in rats.

Liver tissue analyses

Triglycerides

Triglycerides were determined using a Triglyceride Colorimetric Assay Kit (Cayman Chemical, Ann Arbor, MI, USA) according to the manufacturer's protocol (please refer to the supplementary section for more detailed information).

Real-time qPCR

Total RNA from whole liver tissues was extracted using QIAzol Lysis Reagent and RNeasy Kit (Qiagen, Valencia, CA, USA) according to the manufacturer's protocol (please refer to the supplementary section for more detailed information).

Western blot analysis

Proteins from rat liver tissue were homogenized and protein content was determined by the microBCA assay kit (Thermo Fisher Scientific, Waltham, MA, USA) according to the manufacturer's protocol as described in the supplementary section.

OTC enzyme activity

To determine the OTC activity, 10 µg of total protein from human and rat livers was adjusted to 100 µL with water. In brief, samples were incubated in the presence of excessive amounts of L-ornithine and carbamoyl phosphate under optimal enzyme conditions (triethanolamine solution). The enzymatic reaction was stopped by adding a phosphoric acid/sulfuric acid mixture (3:1) and incubating with 3% chromogenic reagent 2,3-Butanedione monoxime. The rate of citrulline production was assessed spectrophotometrically at 490nm (please refer to the supplementary section for more detailed information).

Methylation assay

DNA was isolated from liver tissue using the FitAMP™ DNA isolation kit (P-1003, Epigenetek, Farmingdale, NY, USA). One hundred nanograms of purified DNA was used to assess global methylation using MethylFlash™ Global DNA Methylation (5-mC) ELISA

Easy Kit (P-1034, Epigentek) according to the manufacturer's protocols. Moreover, to investigate whether the OTC promoter was among the methylated regions in HFHC fed rats, the entire coding sequence of the rat OTC gene (Rat - Chromosome X: 13,524,607-13,601,069, reverse strand – Ensemble - ENSRNOT00000004686.3) was screened for CpG islands and putative promoter region using the web interfaces of Ensemble and Promoter 2.0 prediction server. Because of the low-GC content of the genomic regions, the EpiJET™ DNA Methylation Analysis Kit (Thermo Scientific) was employed according to the manufacturer's instructions. Briefly, 0.4 µg purified genomic DNA was incubated at 60°C for 1h with either Epi HpyF30I or Epi TaqI, isoschizomers with TCGA specificity, or left undigested, followed by incubation at 90°C for 10 min. Methylation of cytosine in the TCGA blocks cleavage with Epi HpyF30I but does not affect cleavage with Epi TaqI. Primers for qPCR analysis (Supplementary table 1) were designed using NCBI Primer-BLAST (13) in such a way that amplicons flank/cover the TCGA site, and by taking into account the few data reported in the literature (14-16). Sequences are numerated upstream of the ATG codon. Real time qPCR was performed using Maxima™ SYBR Green qPCR Master Mix (Thermo Scientific) with a two-step cycling protocol for 10 min at 95°C, followed by 35 cycles of 15 s at 95°C and 60 s at 60°C.

Human studies

Subjects, study design and ethics

In humans, we obtained liver biopsies from 20 patients with steatosis and 15 patients with NASH admitted to the Digestive Unit, Valencia, Spain for bariatric surgery. All the patients were operated on by the same surgical team and underwent the identical bariatric intervention, a laparoscopic Roux-en-Y Gastric Bypass. Patients were included if they

were between 18 and 75 years of age. The diagnosis was established by clinical and biochemical findings, and verified by liver biopsy. The patients' baseline characteristics and standard biochemistry have previously been published as part of other studies (17, 18).

We measured blood ammonia levels, liver function tests, markers of metabolic syndrome and C-reactive protein (CRP). In liver tissue, OTC, glutamine synthetase (GS) and cytokeratin (CK)-19 protein levels and enzyme activity, ammonia concentrations, and methylation status of the CPS1 and OTC promoter genes were determined.

Four age-matched patients undergoing liver resection for colorectal metastasis with no history of liver disease were included as controls (mean age 63 (range 53-73) years; mean body mass index (BMI) 27 ± 5 kg/m², ALT 28 ± 12 U/L, aspartate aminotransferase (AST) 23 ± 4 U/L, bilirubin 10 ± 4 μ mol/L, international normalized ratio (INR) 1.1 ± 0.1 , normal glycaemic index). Samples of non-neoplastic liver tissue were collected and processed routinely. These showed no histological signs of steatosis, inflammation or fibrosis. Ethics approvals were obtained from the scientific and ethical committees of the involved hospitals (Hospital Clínic de Valencia, Spain and Royal Free Hospital, UK) and all the participants provided written informed consent in accordance with the Helsinki Declaration.

Liver histology

Histological disease activity was evaluated on formalin-fixed, paraffin-embedded liver sections stained with H&E, and Masson's trichrome. Stained sections were graded by an experienced hepatopathologist according to the NAFLD scoring system proposed by the

National Institute of Diabetes and Digestive and Kidney Disease NASH Clinical Research Network (19). In accordance with the report of the NASH Clinical Research Network, a NAFLD activity score ≥ 5 corresponded in most cases to a diagnosis of NASH, a score of 2 corresponded to “non-NASH” or simple steatosis, while scores of 3 or 4 could reflect either NASH or non-NASH.

Blood analyses

Blood samples for ammonia, ALT, AST, bilirubin, alkaline phosphatase (ALP), INR, albumin, glucose, insulin, hgbA1C, total cholesterol, low-density lipoprotein (LDL) cholesterol, high-density lipoprotein (HDL), triglycerides and CRP were analysed immediately following collection by routine analytical methods. The homeostatic model assessment (HOMA)-index was calculated in accordance with the model (20).

Liver tissue analyses

OTC, GS and CK-19 immunohistochemistry

Tissue samples were placed in 10% neutral-buffered formalin within 1 hour of surgical removal, fixed for 20 hours and paraffin-embedded using standard procedures. Liver sections (4 μm) were deparaffinised in xylene and hydrated through graded alcohols. OTC, GS and CK-19 immunohistochemistry (IHC) was performed as described in the supplementary information.

OTC enzyme activity

OTC enzyme activity was assessed as previously described in relation to the animal experiments.

Ammonia staining

Five μM paraffin embedded sections were deparaffinised in xylene and hydrated through graded alcohols. Sections were washed in distilled water and incubated for 5 minutes with Nessler's reagent, previously filtered with a $0.45 \mu\text{M}$ membrane. The sections were then washed briefly twice in distilled water, counterstained with Mayer's haematoxylin, washed with running tap water, dehydrated in graded alcohols and mounted with DPX permanent mounting medium (21).

Immunohistochemistry imaging quantification

OTC IHC was quantified using the Open Source Plugin for the Quantitative Evaluation optimised by Varghese et al. (22). For further information please refer to the supplementary information section.

Methylation assay

Human methylation analyses were carried out by EpigenDx (Hopkinton, MA, USA). Briefly, human genomic DNA was bisulfite converted to modify unmethylated cytosines to uracils. Subsequently, library construction, amplification and enrichment of +/- 1 region of CPS1 and -2.4kb kb of OTC from the transcriptional start sites were performed. The resulting PCR amplicons went through a tagmentation process. Subsequently, the libraries were sequenced and reads mapped to the reference sequence, and the relative proportion of methylated and unmethylated alleles at each CpG site was determined. Thirty seven CpG

islands for CPS1 and 22 for OTC were found, sequenced and analysed (Supplementary Table 2).

***In vitro* studies**

All experiments were approved by the Laboratory Animal Care and Use Committee of the University of Barcelona and were conducted in accordance with the European Community guidelines for the protection of animals used for experimental and other scientific purposes (European Economic Community (EEC) Directive 86/609).

Primary hepatocytes were isolated from male Wistar rats (n=4, 300-350g) (Charles River, Sant Cugat del Vallès, Spain) and cultured as described in the supplementary information. Bovine serum albumin (BSA) and free fatty acid (FFA) solutions (palmitate acid and oleate acid) were prepared as described in detail in the supplementary section. Hepatocytes were seeded in collagen 6 well plates for 4h after the isolation with a medium containing 10% of FBS. Dead hepatocytes were removed by extensive wash and left overnight with 2% FBS medium. The next day, cells were incubated with FFAs. After 48 and 72 hours, respectively, lipid accumulation in the hepatocytes was quantified using Oil-red-O staining as described in the supplementary information.

Methylation analyses of two regions in the OTC promoter and real-time qPCR for CPS1 and OTC were performed as described in the section under animal experiments except that 0.4 µg of RNA was used for cell analyses.

Ammonia levels were measured in the supernatant using standard methods at the Hospital Clinic of Barcelona's CORE laboratory.

Statistical analysis

Statistical analysis was performed using Stata 11.1 software (Stata Corporation, College Station, TX). In the animal study, continuous variables were analysed using Kruskal-Wallis rank test and histology scores using Fisher's exact test. When significant, post-hoc tests for continuous variables were performed among groups by the Mann-Whitney test and histology scores using Fisher's exact test. In the human study, the assumption of normality was checked using quantile-quantile plots (Q-Q plots) and histograms to ensure normally distributed variables. Differences between normally distributed patient characteristics were evaluated by Student's t-test. Pearson's χ^2 test was used to compare categorical variables. Some variables showed skewed distributions with variance heterogeneity, but after log₁₀ transformation most variables were considered normally distributed with variance homogeneity, and Student's t-test was performed on the transformed data. However, NAFLD score, fibrosis score, bilirubin, INR and glucose were evaluated by the Mann-Whitney test. When comparing the differences between patients with steatosis and NASH, and controls, the data were analysed using ANOVA; when significant, post-hoc tests were performed among groups by Student's t-test. In the *in vitro* study, differences between the groups were analysed using Kruskal-Wallis rank test. When significant, post-hoc tests were performed among groups by the Mann-Whitney test. Normally distributed data are presented as mean \pm SD and log-transformed and non-parametric tested data are presented as median (IQR). P-values <0.05 were considered statistically significant.

RESULTS

Animal study

Animal characteristics

After 10 and 12 months, the liver weight increased threefold in the HFHC animals compared with controls (NC) ($P < 0.01$) and was reduced 30% after changing the diet back to normal chow ($P < 0.05$). In addition, the spleen weight increased after 10 and 12 months in HFHC-fed animals ($P < 0.05$ and $P < 0.01$, respectively) and insignificantly decreased after changing back to normal chow ($P = 0.20$), Table 1.

Plasma ALT was increased in HFHC animals compared with controls (10 months: $P < 0.01$, 12 months: $P < 0.05$) and normalised when changed back to normal chow ($P < 0.01$). Similarly, albumin decreased in HFHC animals (10 months: $P < 0.05$, 12 months: $P < 0.01$) and insignificantly increased on normal chow ($P = 0.14$). Total cholesterol was markedly increased in HFHC animals ($P < 0.01$, 10 and 12 months) and decreased when changed back to normal chow ($P < 0.01$), Table 1.

Macroscopically, the livers from HFHC-fed rats were enlarged and pale yellow. Microscopically, HFHC-group livers showed severe steatosis, with varying degrees of hepatocyte ballooning, inflammation and fibrosis. Overall, most of the HFHC animals showed histological evidence of NASH. Similar histological changes continued to be present in the livers of animals that had reverted to normal chow, but there was non-statistically significant improvement in hepatocyte ballooning, Table 1. Histologically, livers from control animals were entirely normal. Liver triglycerides were significantly increased in

HFHC animals compared with controls and tended to decrease after changing back to normal chow but these changes were not statistically significant, Table 1.

UCE gene expression

In the HFHC animals, gene expression of OTC was reduced significantly compared with control animals ($P < 0.01$, both). Changing the HFHC diet to normal chow restored OTC gene expression ($P = 0.03$). In addition, CPS1 gene expression decreased in HFHC animals compared with controls ($P < 0.05$, both). No differences were observed between groups in ASS, ASL or ARG gene expression (Figure 1).

OTC and CPS protein expression

Amongst the 5 UCes, only OTC and CPS1 showed marked reduction at the mRNA level in the HFHC animals compared with controls. This was further confirmed at the protein expression level for OTC and CPS1, demonstrating that both proteins were affected in HFHC animals and not in controls. In addition, by changing the HFHC diet to normal chow OTC and CPS1 protein levels were restored (Figure 2A, B).

OTC enzyme activity

OTC enzyme activity was significantly reduced in the HFHC animals compared with controls, both after 10 months (0.18 ± 0.03 vs. 0.34 ± 0.06 nmol/min/ μ g protein; $P < 0.01$) and 12 months (0.18 ± 0.02 vs. 0.33 ± 0.05 nmol/min/ μ g protein; $P < 0.01$). OTC enzyme activity was restored when changing the diet to normal chow (0.26 ± 0.04 vs. 0.18 ± 0.02 nmol/min/ μ g protein; $P < 0.01$; Figure 2C).

Methylation

Initially, we quantified the global DNA methylation in all our groups. No statistically significant differences were observed (Supplementary Figure 1). On further investigation of the region upstream of OTC start codon, we observed an increase in %5-mC for region 1 (between -436F and -175R bp) and region 2 (between -216F and -67R bp) in the HFHC animals compared with controls, both after 10 months (region 1: 6.7 ± 1.8 vs. 2.7 ± 1.2 %5-mC, $P=0.02$; region 2: 2.6 ± 0.7 vs. 0.7 ± 0.4 %5-mC, $P=0.02$) and 12 months (region 1: 7.4 ± 0.9 vs. 3.1 ± 1.3 %5-mC, $P=0.02$; region 2: 2.3 ± 1.0 vs. 0.5 ± 0.4 %5-mC, $P=0.02$). Reversal of NASH by changing the diet to normal chow reduced %5-mC in region 1 (5.6 ± 0.7 vs. 7.4 ± 0.9 %5-mC, $P=0.04$; Figure 3).

Human studies

Patients

Demographic, clinical, histological and biochemical characteristics of patients are listed in Supplementary table 3. Twenty patients with steatosis (age 44 ± 9 years; 16 women (80%); BMI 49 ± 8) and 15 patients with NASH (age 51 ± 6 years; 13 women (87%); BMI 49 ± 8) were included prospectively. Expectedly, the NAFLD score was higher in patients with NASH compared with patients with steatosis (6 (6-7) vs. 1 (1-1), $P<0.001$). Also, the fibrosis score was higher in NASH compared with steatotic patients (3 (1-3) vs. 0 (0-0), $P<0.001$).

Glutamine synthetase staining

GS protein levels were assessed by IHC. GS positive cells were found around the pericentral area in healthy controls, whereas GS concentrations progressively decreased

in steatosis and NASH patients (Figure 4A). Its localisation was still in the pericentral area in steatosis patients but had lost this pericentral zonation in patients with NASH.

OTC staining and enzyme activity

OTC protein levels were assessed by IHC. Healthy controls showed a periportal distribution of cytoplasmic immunoreactivity for OTC. A few stained hepatocytes with massive lipid droplet content and no zonal pattern were detected in patients with steatosis, and a complete lack of zonal distribution pattern was observed in samples from patients with NASH (Figure 4B). A progressive decrease in OTC staining was observed with a 50% reduction in steatosis patients compared with controls ($P=0.003$) and a further 50% reduction in NASH patients compared with steatosis patients ($P=0.004$; Figure 4C).

The OTC enzyme activity was markedly decreased in patients with steatosis ($0.045 \pm 0.039 \mu\text{mol}/\text{min}/\mu\text{g}$) and NASH ($0.059 \pm 0.040 \mu\text{mol}/\text{min}/\mu\text{g}$) compared with the controls ($0.268 \pm 0.061 \mu\text{mol}/\text{min}/\mu\text{g}$), $P<0.0001$, both. No difference in OTC enzyme activity was observed between patients with steatosis and NASH (Figure 4D).

Ammonia levels

Patients with NASH had increased plasma ammonia levels ($112 \pm 35 \mu\text{M}$) compared with patients with steatosis (87 ± 24 ; $P=0.01$; Figure 5D). Nessler's staining in human liver samples showed a 5-fold increase in ammonia concentrations in steatosis patients compared with controls ($P<0.0001$) and a further 2-fold increase in NASH compared with steatosis patients ($P<0.001$; Figure 5C). Nessler's reagent showed accumulation of ammonia in NASH patients with brown/black precipitates where inflammatory foci were

present (Figure 5B). Comparison of the site of ammonia staining with that of GS and CK-19 staining (Figure 5A) to localise the bile ducts suggested that ammonia was distributed ubiquitously in the liver lobule without any specific distribution.

Methylation

CpGs islands at -1564, -1561, -969 and -960bp from the start codon of CPS1 were hypermethylated in NASH compared with controls and steatosis patients (9 vs. 5; 11 vs. 4; 7 vs. 4; 6 vs. 3% of methylation, respectively, Figure 6A). For OTC, CpGs island at -647, -360, -354 and -295bp upstream of the start codon showed high levels of methylation in NASH patients compared with controls and steatosis patients (28 vs. 12; 25 vs. 14; 71 vs. 61; 64 vs. 48% of methylation, respectively, Figure 6B). Interestingly, the overall % of methylation for the entire region under analysis was higher for OTC compared with CPS1. Furthermore, the hypermethylated region of the OTC gene in NASH patients overlapped with the hypermethylated region in HFHC fed rats (from -647 to -295bp and from 436 to -67bp, respectively) located on chromosome X in both species.

***In vitro* study in primary rat hepatocytes**

After incubation with FFA mixture, lipid droplets were visible intracellularly and tended to accumulate around the nuclei (Figure 7A). Oil-red-O staining reached the highest reading after 48h incubating with a 200 μ M FFA concentration (48h 200 μ M vs. 48h non-treated; $p=0.02$; Figure 7B).

The previously described region 1 and 2 upstream of the OTC start codon were both found to be hypermethylated 48 and 72h after incubation with all three concentrations of FFA

mixture (48+72h 100/200/400 μ M vs. 48+72h NT, respectively; $p=0.02-0.04$; Figure 7C+D). OTC and CPS1 showed a reduction at the mRNA level 48 and 72 hours after treatment with the 400 μ M FFA mixture compared with non-treated cells (48+72h 400 μ M vs. 48+72h NT, respectively; $p=0.02-0.04$; Figure 7E+F).

In the supernatant, ammonia concentration increased significantly after both 48 and 72 hours and at all three concentrations of FFA mixture (48+72h 100/200/400 μ M vs. 48+72h NT, respectively; $p=0.02$ all; Figure G).

DISCUSSION

We show for the first time that, even in the absence of cirrhosis, both experimental and clinical NASH are associated with a reduction in gene and protein expression of the UCEs OTC and CPS1, these functional changes being associated with hyperammonemia. In the animal model, both the gene and protein expression changes, and the abnormal OTC activity, were restored with dietary intervention, this being accompanied by biochemical improvement and a decrease in liver fat. We were able to recapitulate the results of the *in vivo* experiment in an *in vitro* model of steatosis that was induced in primary rat hepatocytes. The data showed that induction of progressive hepatocyte steatosis was associated with a significant and a dose dependent reduction in the gene expression of OTC and CPS1 with evidence of hypermethylation of these genes as observed *in vivo*. This reduction in gene expression and hypermethylation was associated with significantly greater and dose dependent increase in ammonia concentration in the supernatant of the steatotic hepatocytes suggesting that steatosis is likely to be causal rather than a mere association.

Histologically, dietary intervention resulted in a decrease in ballooning, but not in either steatosis or inflammation, suggesting that restoration of UCE expression and activity precedes improvement in histological appearances. The lack of full histological recovery may be explained by a temporary increase in the production of endogenous fatty acids in the liver to make up for the fat missing in the diet (23) and the increase in inflammation is likely an earlier described consequence of the sudden change in calorie intake (23, 24). This suggests that components of the diet (e.g. free fatty acids, cholesterol) may have a direct effect on the regulation of the mitochondrial UCEs. Fatty acids undergo β -oxidation

in the mitochondria for production of cellular energy and the increased fatty acid load on the liver might disrupt mitochondrial function, thereby affecting OTC and CPS1 function. In NAFLD patients, epigenetic modifications of liver mitochondrial DNA have been shown to decrease transcriptional activity and protein expression of NADH dehydrogenase 6, resulting in mitochondrial dysfunction (25). Dysfunctional mitochondria can send signals to the nucleus to alter gene expression to modify cellular function and reprogram cell metabolism. This retrograde communication helps cellular adaptation to various stressors such as massive cytosolic lipid accumulation (26, 27).

Our *in vitro* studies provide further support for our suggestion that hypermethylation of the promoter regions of UCE genes may be the operative mechanism of the observed changes in UCEs induced by steatosis. We demonstrate that accumulation of lipids in rat hepatocytes from medium fatty acids induces hypermethylation of the OTC promoter gene and eventually a decrease in the gene expression of urea cycle enzymes and an increase in ammonia concentrations in the culture medium. In keeping with this observation, long-chain fatty acids have previously been found to suppress UCE gene expression *in vitro* (28). Previous studies focussing on the methylome in NAFLD patients with early or severe disease have shown that over 60,000 CpG sites are differentially methylated contributing to differences in gene expression (29, 30). The mechanism of how induction of steatosis results in increased methylation of the UCE genes have not been clarified in this study.

Our studies extend these observations by demonstrating that in patients with steatosis and NASH, hypermethylation of the promoter region of the CPS1 and OTC genes may be the operative mechanism of the observed changes in gene expression and function. It has

been suggested that epigenetic processes such as DNA methylation mediate the effects of environmental factors, including a western-style diet, on the development and progression of NAFLD (31). Epigenetic alterations are known to be involved in lipid metabolism, endoplasmic reticulum stress, mitochondrial damage, oxidative stress and inflammation (31). In a mouse model, high-fat-sucrose diet induced steatosis was associated with methylation of total DNA and specific gene promoters in the liver (32). Moreover, in humans with NAFLD, altered methylation of genes involved in the development of steatohepatitis and fibrosis was observed, and its severity differentiated between mild and advanced NAFLD, suggesting a role for DNA methylation in the progression of NAFLD (25, 30, 33). These changes were reversible after bariatric surgery and weight loss, by remodelling of the epigenetic signature (29). Given these observations, it is possible that altered DNA methylation may also be the regulatory mechanism of urea synthesis, through differential gene expression of OTC and CPS1. DNA methylation is more likely associated with transcriptional repression when present at the promoter regions of the genes and it follows that higher levels of DNA methylation around gene promoters correlate with low or no transcription, thereby regulating the activity of the genes (34). Therefore, we studied sites upstream of the start codon of the relevant promoter genes and found several regions that were hypermethylated, suggesting that altered DNA methylation could be the regulatory mechanism behind decreased urea synthesis in NASH. In keeping with this observation, a proteomic study showed down regulation of CPS1 in patients with NASH (35).

The reduction in UCE expression and activity was associated with increased ammonia levels, which has also been observed by Felipo et al. (17). It is noteworthy that the NASH

patients had higher ammonia levels compared with patients with simple steatosis, whereas no differences in OTC protein expression and enzyme activity were observed. This observation is consistent with the fact that DNA methylation of CPS1 was more marked in patients with NASH compared with those with steatosis. CPS1 is the flux-generating urea cycle feeder enzyme which under physiological conditions, controls influx to the cycle. As CPS1 is also localized in the mitochondria and has previously been found to be down-regulated in NASH patients (35), it is likely that the NASH patients had a more pronounced reduction in CPS1 activity, causing a further functional down-regulation of ureagenesis and, ultimately, hyperammonemia. Also, hepatic GS protein expression was more reduced in NASH patients, which most likely contributes to the high ammonia levels. This hypothesis will need to be studied.

The data we present demonstrating that hyperammonemia is a feature of early stages of NAFLD has potential implications for the treatment of the disease. We have shown in previous studies that chronic exposure to high levels of ammonia has a profound effect on HSC activation status and that its removal impacts positively on the HSC's phenotype *in vitro* and *in vivo*. We suggest that ammonia removal in NASH patients would lead to a more quiescent HSC phenotype and slow the progression of NAFLD. In preliminary studies, the administration of OCR-002, a drug known to reduce ammonia concentration, prevented progression of fibrosis (36). Furthermore, patients with NAFLD have been shown to have hyperammonemia and neuropsychological disturbances (17), although the mechanism underlying this has so far not been clarified.

In conclusion, steatosis in rats and humans is associated with reversible changes in UCEs that result in hyperammonemia, possibly through hypermethylation of UCE genes and impairment of urea synthesis. These data could be reproduced in an *in vitro* model of hepatocyte steatosis suggesting that the steatosis induced changes in UCE were likely to be causal rather than a mere association. As hyperammonemia can cause progression of liver injury and fibrosis, these findings support a strategy of targeting ammonia as a potential treatment for NASH.

ACCEPTED MANUSCRIPT

ACKNOWLEDGEMENTS

This study was generously supported by grants from the Novo Nordisk foundation, the Danish Council for Independent Research, and Ministerio de Ciencia e Innovación (SAF2014-51851-R to V.F., and FIS PI15/00035 ISCIII to C.M.).

ACCEPTED MANUSCRIPT

REFERENCES

1. Williams R, Horton R. Liver disease in the UK: a Lancet Commission. *Lancet* 2013;382:1537-1538.
2. Blachier M, Leleu H, Peck-Radosavljevic M, Valla DC, Roudot-Thoraval F. The burden of liver disease in Europe: a review of available epidemiological data. *J Hepatol* 2013;58:593-608.
3. Matteoni CA, Younossi ZM, Gramlich T, Boparai N, Liu YC, McCullough AJ. Nonalcoholic fatty liver disease: a spectrum of clinical and pathological severity. *Gastroenterology* 1999;116:1413-1419.
4. Tariq Z, Green CJ, Hodson L. Are oxidative stress mechanisms the common denominator in the progression from hepatic steatosis towards non-alcoholic steatohepatitis (NASH)? *Liver Int* 2014;34:e180-190.
5. Ekstedt M, Hagstrom H, Nasr P, Fredrikson M, Stal P, Kechagias S, Hultcrantz R. Fibrosis stage is the strongest predictor for disease-specific mortality in NAFLD after up to 33 years of follow-up. *Hepatology* 2015;61:1547-1554.
6. Angulo P, Kleiner DE, Dam-Larsen S, Adams LA, Bjornsson ES, Charatcharoenwittaya P, Mills PR, et al. Liver Fibrosis, but No Other Histologic Features, Is Associated With Long-term Outcomes of Patients With Nonalcoholic Fatty Liver Disease. *Gastroenterology* 2015;149:389-397 e310.
7. Rombouts K, Marra F. Molecular mechanisms of hepatic fibrosis in non-alcoholic steatohepatitis. *Dig.Dis.* 2010;28:229-235.
8. Shambaugh GE, 3rd. Urea biosynthesis I. The urea cycle and relationships to the citric acid cycle. *American Journal of Clinical Nutrition* 1977;30:2083-2087.
9. Pessayre D, Fromenty B. NASH: a mitochondrial disease. *Journal of Hepatology* 2005;42:928-940.
10. Thomsen KL, Gronbaek H, Glavind E, Hebbard L, Jessen N, Clouston A, George J, et al. Experimental nonalcoholic steatohepatitis compromises ureagenesis, an essential hepatic metabolic function. *Am J Physiol Gastrointest Liver Physiol* 2014;307:G295-301.
11. Jalan R, De Chiara F, Balasubramanian V, Andreola F, Khetan V, Malago M, Pinzani M, et al. Ammonia produces pathological changes in human hepatic stellate cells and is a target for therapy of portal hypertension. *J Hepatol* 2016;64:823-833.
12. Bedossa P, Poitou C, Veyrie N, Bouillot JL, Basdevant A, Paradis V, Tordjman J, et al. Histopathological algorithm and scoring system for evaluation of liver lesions in morbidly obese patients. *Hepatology* 2012;56:1751-1759.
13. Ye J, Coulouris G, Zaretskaya I, Cutcutache I, Rozen S, Madden TL. Primer-BLAST: A tool to design target-specific primers for polymerase chain reaction. *BMC Bioinformatics* 2012;13:134.
14. Takiguchi M, Murakami T, Miura S, Mori M. Structure of the rat ornithine carbamoyltransferase gene, a large, X chromosome-linked gene with an atypical promoter. *Proc Natl Acad Sci U S A* 1987;84:6136-6140.
15. Murakami T, Nishiyori A, Takiguchi M, Mori M. Promoter and 11-kilobase upstream enhancer elements responsible for hepatoma cell-specific expression of the rat ornithine transcarbamylase gene. *Mol Cell Biol* 1990;10:1180-1191.
16. Nishiyori A, Tashiro H, Kimura A, Akagi K, Yamamura K, Mori M, Takiguchi M. Determination of tissue specificity of the enhancer by combinatorial operation of tissue-enriched transcription factors. Both HNF-4 and C/EBP beta are required for liver-specific activity of the ornithine transcarbamylase enhancer. *J Biol Chem* 1994;269:1323-1331.

17. Felipo V, Urios A, Montesinos E, Molina I, Garcia-Torres ML, Civera M, Olmo JA, et al. Contribution of hyperammonemia and inflammatory factors to cognitive impairment in minimal hepatic encephalopathy. *Metabolic Brain Disease* 2012;27:51-58.
18. Felipo V, Urios A, Garcia-Torres ML, El Mlili N, del Olmo JA, Civera M, Ortega J, et al. Alterations in adipocytokines and cGMP homeostasis in morbid obesity patients reverse after bariatric surgery. *Obesity (Silver Spring)* 2013;21:229-237.
19. Kleiner DE, Brunt EM, Van Natta M, Behling C, Contos MJ, Cummings OW, Ferrell LD, et al. Design and validation of a histological scoring system for nonalcoholic fatty liver disease. *Hepatology* 2005;41:1313-1321.
20. Matthews DR, Hosker JP, Rudenski AS, Naylor BA, Treacher DF, Turner RC. Homeostasis model assessment: insulin resistance and beta-cell function from fasting plasma glucose and insulin concentrations in man. *Diabetologia* 1985;28:412-419.
21. Gutierrez-de-Juan V, Lopez de Davalillo S, Fernandez-Ramos D, Barbier-Torres L, Zubiete-Franco I, Fernandez-Tussy P, Simon J, et al. A morphological method for ammonia detection in liver. *PLoS One* 2017;12:e0173914.
22. Varghese F, Bukhari AB, Malhotra R, De A. IHC Profiler: An Open Source Plugin for the Quantitative Evaluation and Automated Scoring of Immunohistochemistry Images of Human Tissue Samples. *PLOS ONE* 2014;9:e96801.
23. Sanyal AJ, American Gastroenterological A. AGA technical review on nonalcoholic fatty liver disease. *Gastroenterology* 2002;123:1705-1725.
24. Luyckx FH, Desai C, Thiry A, Dewe W, Scheen AJ, Gielen JE, Lefebvre PJ. Liver abnormalities in severely obese subjects: effect of drastic weight loss after gastroplasty. *Int J Obes Relat Metab Disord* 1998;22:222-226.
25. Pirola CJ, Gianotti TF, Burgueno AL, Rey-Funes M, Loidl CF, Mallardi P, Martino JS, et al. Epigenetic modification of liver mitochondrial DNA is associated with histological severity of nonalcoholic fatty liver disease. *Gut* 2013;62:1356-1363.
26. Quiros PM, Mottis A, Auwerx J. Mitonuclear communication in homeostasis and stress. *Nat Rev Mol Cell Biol* 2016;17:213-226.
27. Ghezzi D, Zeviani M. Assembly factors of human mitochondrial respiratory chain complexes: physiology and pathophysiology. *Adv Exp Med Biol* 2012;748:65-106.
28. Tomomura M, Tomomura A, Dewan MA, Saheki T. Long-chain fatty acids suppress the induction of urea cycle enzyme genes by glucocorticoid action. *FEBS Lett* 1996;399:310-312.
29. Ahrens M, Ammerpohl O, von Schonfels W, Kolarova J, Bens S, Itzel T, Teufel A, et al. DNA methylation analysis in nonalcoholic fatty liver disease suggests distinct disease-specific and remodeling signatures after bariatric surgery. *Cell Metab* 2013;18:296-302.
30. Murphy SK, Yang H, Moylan CA, Pang H, Dellinger A, Abdelmalek MF, Garrett ME, et al. Relationship between methylome and transcriptome in patients with nonalcoholic fatty liver disease. *Gastroenterology* 2013;145:1076-1087.
31. Sun C, Fan JG, Qiao L. Potential epigenetic mechanism in non-alcoholic Fatty liver disease. *Int J Mol Sci* 2015;16:5161-5179.
32. Cordero P, Campion J, Milagro FI, Martinez JA. Transcriptomic and epigenetic changes in early liver steatosis associated to obesity: effect of dietary methyl donor supplementation. *Mol Genet Metab* 2013;110:388-395.
33. Zeybel M, Hardy T, Robinson SM, Fox C, Anstee QM, Ness T, Masson S, et al. Differential DNA methylation of genes involved in fibrosis progression in non-alcoholic fatty liver disease and alcoholic liver disease. *Clin Epigenetics* 2015;7:25.
34. Bird A. DNA methylation patterns and epigenetic memory. *Genes Dev* 2002;16:6-21.

35. Rodriguez-Suarez E, Duce AM, Caballeria J, Martinez Arrieta F, Fernandez E, Gomara C, Alkorta N, et al. Non-alcoholic fatty liver disease proteomics. *Proteomics Clin Appl* 2010;4:362-371.
36. De Chiara F, Habtension A, Davies N, Andreola F, Rombouts K, Arias N, Thomsen KL, et al. Early increase in ammonia is a feature of Non-Alcoholic Fatty Liver Disease and the ammonia lowering drug, Ornithine Phenylacetate (OCR-002) prevents progression of fibrosis in a rodent model. Abstract, The International Liver Congress. 2017.

ACCEPTED MANUSCRIPT

Table 1. Clinical, biochemical and histologic characteristics of the animal models.

	10 months		12 months			P values comparing all groups
	Control	HFHC	Control	HFHC	Changed back	
Whole BW, start (g)	202 (201-213)	206 (203-213)	205 (203-208)	208 (200-209)	209 (201-211)	P=0.94
Whole BW, end (g)	297 (284-305)	279 (249-306)	325 (310-352)	309 (286-316)	318 (301-335)	P=0.04
Weight gain (g)	85 (79-104)	78 (45-92)	120 (106-138)	98 (82-116)	107 (101-123)	P=0.01
Liver weight (g)	6.3 (6.1-6.6)	21.0 (18.7-26.1)**	7.1 (6.8-7.5)	19.8 (15.0-23.6)**	14.6 (11.1-15.1)**#	P<0.001
Liver/body weight	2.2 (2.1-2.3)	7.5 (6.4-9.7)**	2.2 (2.1-2.3)	6.4 (5.5-7.5)**	4.5 (3.7-5.2)**#	P<0.001
Spleen weight (g)	0.6 (0.6-0.7)	1.4 (1.0-1.5)*	0.7 (0.6-0.7)	1.2 (1.0-1.3)**	1.0 (0.9-1.0)**	P<0.01
ALT (U/L)	36 (24-50)	105 (83-132)**	27 (24-53)	70 (65-85)*	17 (9-29)##	P<0.001
Bilirubin (µmol/L)	5 (5-5)	5 (5-5)	5 (5-5)	5 (5-5)	5 (5-5)	P=0.56
Albumin (g/L)	16 (15-17)	14 (14-15)*	17 (15-18)	14 (13-14)**	15 (14-17)	P<0.01
Glucose (mmol/L)	4.0 (3.9-4.4)	4.2 (4.0-4.3)	4.3 (3.8-4.3)	4.7 (4.5-4.8)	4.3 (4.2-4.8)	P=0.08
Total cholesterol (mmol/L)	1.6 (1.2-2.4)	16.7 (13.9-20.2)**	2.2 (1.8-2.5)	10.2 (10.1-14.1)**	5.2 (4.1-5.3)**##	P<0.001
Triglyceride (mmol/L)	1.1 (0.6-1.1)	1.5 (0.8-1.6)	1.1 (1.0-1.3)	1.1 (1.0-1.1)	0.9 (0.7-0.9)	P=0.49
Steatosis (0/1/3) n	4/2/0	0/0/6**	5/1/0	0/0/6**	0/0/6**	P<0.001
Ballooning (0/1/2) n	6/0/0	2/2/2	6/0/0	2/1/3	2/4/0*	P<0.01
Inflammation (0/1/2) n	6/0/0	0/1/5**	5/1/0	0/5/1*	0/0/6**##	P<0.001
Fibrosis (0/1/2) n	6/0/0	3/2/1	6/0/0/0	1/5/0**	0/3/3**	P<0.001
Liver triglyceride (% control mean)	97 (78-117)	212 (179-236)	102 (77-122)	155 (112-174)	121 (105-146)	P=0.15

*P<0.05 compared with control

#P<0.05 compared with HFHC

**P<0.01 compared with control

##P<0.01 compared with HFHC

***P<0.001 compared with control

###P<0.001 compared with HFHC

Data are presented as median (IQR)

Body, liver and spleen weight, plasma concentrations of alanine aminotransferase (ALT), bilirubin, albumin, glucose, total cholesterol and triglycerides, histology scores and liver triglycerides in control animals (10 (n=5) & 12 (n=6) months), high-fat high-cholesterol (HFHC) fed animals (10 (n=5) & 12 (n=6) months) and HFHC fed animals changed back to standard diet after 10 months (12 months, n=6). Continuous variables were analysed using Kruskal-Wallis rank test and histology scores using Fisher's exact test. When significant, post-hoc tests for continuous variables were performed among groups by the Mann-Whitney test and histology scores using Fisher's exact test.

ACCEPTED MANUSCRIPT

FIGURE LEGENDS

Figure 1.

Urea cycle enzymes mRNA levels.

Changes in the mRNA levels of ornithine transcarbamylase (OTC) (A), carbamoyl phosphate synthetase 1 (CPS1) (B), argininosuccinate synthetase (ASS) (C), argininosuccinate lyase (ASL) (D) and arginase (ARG) (E) in liver tissue from control animals (NC, 10 (n=5) & 12 (n=6) months), high-fat high-cholesterol (HFHC) fed animals (10 (n=5) & 12 (n=6) months), and HFHC fed animals changed back to normal chow after 10 months (HFHC10+NC2, n=6). Results are presented as relative levels compared with 10 month control rats. Data were analysed using Kruskal-Wallis rank test and when significant, post-hoc tests were performed among groups by the Mann-Whitney test. The solid horizontal lines indicate the mean values and the error bars SD.

Figure 2.

Ornithine transcarbamylase protein expression and activity (A+C) and carbamoyl phosphate synthetase 1 protein expression (B).

Protein expression and enzyme activity of ornithine transcarbamylase (OTC) and protein expression of carbamoyl phosphate synthetase 1 (CPS1) in liver tissue from control animals (NC, 10 & 12 months, n=6), high-fat high-cholesterol (HFHC) fed animals (10 & 12 months, n=6) and HFHC fed animals changed back to normal chow after 10 months (HFHC10+NC2, n=6). In the protein expression analyses, the samples from the 6 rat livers per group were pooled and presented as columns representing the mean. The OTC enzyme activity is shown as solid horizontal lines indicating the mean values and the error

bars SD. The five groups were compared using Kruskal-Wallis rank test and when significant, post-hoc tests were performed among groups by the Mann-Whitney test..

Figure 3. Ornithine transcarbamylase promoter gene methylation

Methylation of the ornithine transcarbamylase promoter gene for region 1 (-436F -175R) and region 2 (-216F -67R) in liver tissue from control animals (NC, 10 & 12 months, n=4), high-fat high-cholesterol (HFHC) fed animals (10 & 12 months, n=4) and HFHC fed animals changed back to normal chow after 10 months (HFHC10+NC2, n=4). The five groups were compared using Kruskal-Wallis rank test and when significant, post-hoc tests were performed among groups by the Mann-Whitney test. The solid horizontal lines represent the mean values and the error bars SD.

Figure 4. Glutamine synthetase (A) and ornithine transcarbamylase protein expression levels (B+C) and enzyme activity (D) in liver tissue

Glutamine synthetase (GS) (A) and ornithine transcarbamylase (OTC) (B & C, n=5 in patient groups) protein expression levels assessed by immunohistochemistry and OTC enzyme activity (D) in liver tissue from controls (n=4) and from patients with steatosis (n=20) and non-alcoholic steatohepatitis (NASH; n=15). Arrows point to positive immunoreactivity to GS and OTC. Differences between controls, steatosis and NASH patients were analysed using ANOVA; when significant, post-hoc tests were performed among groups by Student's t-test. The solid horizontal lines indicate the mean values and the error bars SD.

Figure 5. Cytokeratin-19 protein expression levels (A) and ammonia (B+C)

in liver tissue and plasma ammonia levels (D)

Cytokeratin (CK)-19 protein expression levels assessed by immunohistochemistry (A). Ammonia levels in liver tissue from controls and in patients with steatosis and NASH assessed using Nessler's reagent (n=5) (B & C). Black arrows point to ammonia and pink arrows to inflammatory foci. Plasma ammonia levels in patients with steatosis (n=20) and non-alcoholic steatohepatitis (NASH) (n=15) (D). Differences in liver ammonia levels between controls, steatosis and NASH patients were analysed using ANOVA; when significant, post-hoc tests were performed among groups by Student's t-test. Differences in plasma ammonia levels between steatosis and NASH patients were analysed by Student's t-test. The solid horizontal lines indicate the mean values and the error bars SD.

Figure 6. Carbamoyl phosphate synthetase 1 (A) and Ornithine transcarbamylase (B) promoter gene methylation

Methylation of the carbamoyl phosphate synthetase 1 (CPS1) (A) and ornithine transcarbamylase (OTC) (B) promoter genes in liver tissue from healthy controls and patients with steatosis and non-alcoholic steatohepatitis (NASH) (n=3). The columns indicate the mean values and the error bars SD.

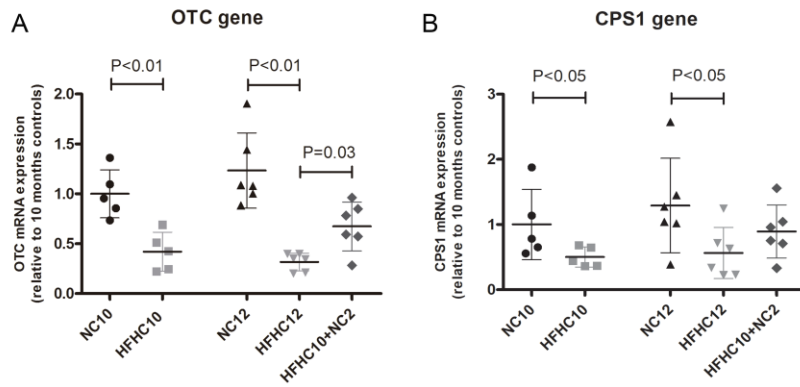
Figure 7. Lipid accumulation (A+B), ornithine transcarbamylase promoter gene methylation (C+D), ornithine transcarbamylase (E) and carbamoyl phosphate synthetase 1 (F) gene expression in primary rat hepatocytes and supernatant ammonia levels (G).

Representative Oil-red-O staining (A), quantification of lipid accumulation (B) and changes in methylation of the ornithine transcarbamylase promoter gene for region 1 (-436F -175R) (C) and region 2 (-216F -67R) (D), mRNA levels of ornithine transcarbamylase (OTC) (E)

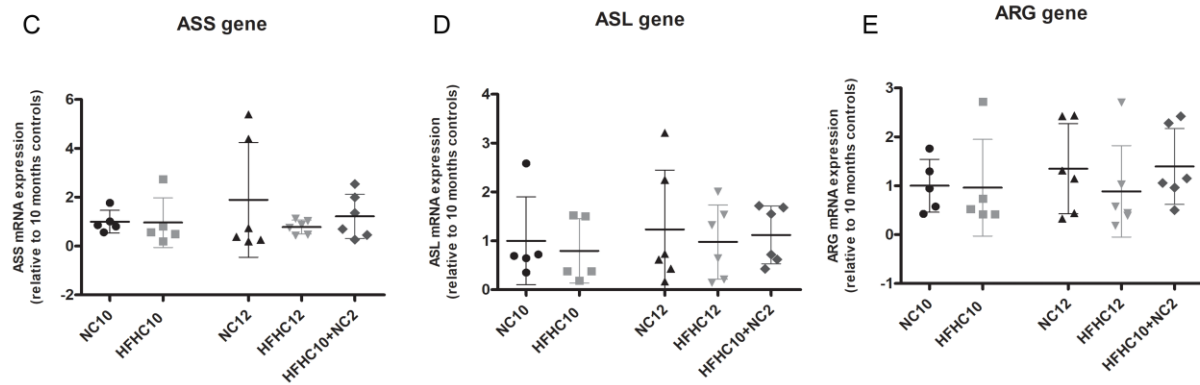
and carbamoyl phosphate synthetase 1 (CPS1) (F) in non-treated (NT) primary rat hepatocytes and after incubation with three different concentrations of free fatty acids (FFAs) for 48 and 72 hours, and ammonia levels in the culture medium (G) (n=4). Data were analysed using Kruskal-Wallis rank test and when significant, post-hoc tests were performed among groups by the Mann-Whitney test. The columns indicate the mean values and the error bars SD.

Figure 1

Location of the enzyme: mitochondria



Location of the enzyme: cytosol



ACCEPTED MANUSCRIPT

Figure 2

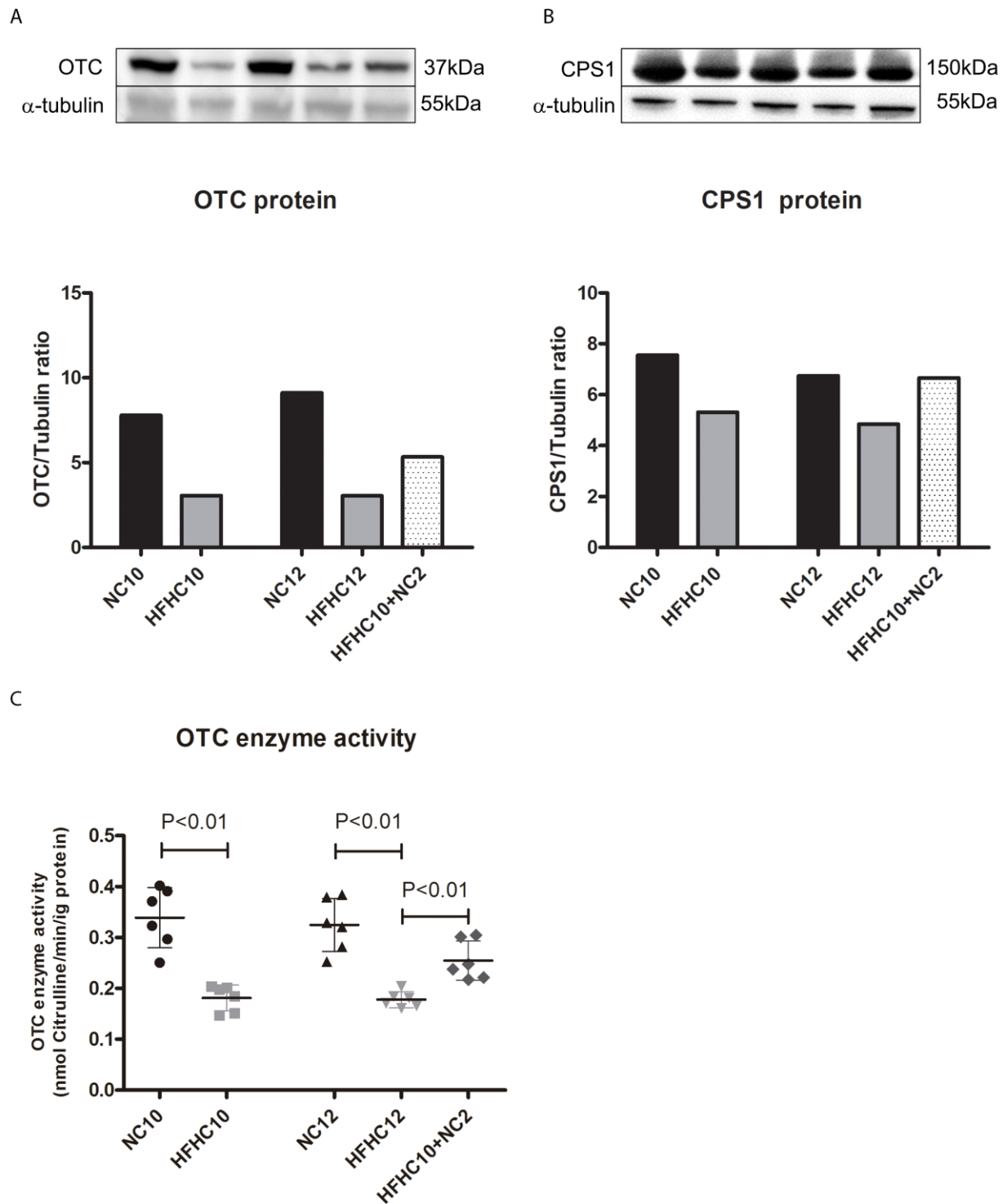
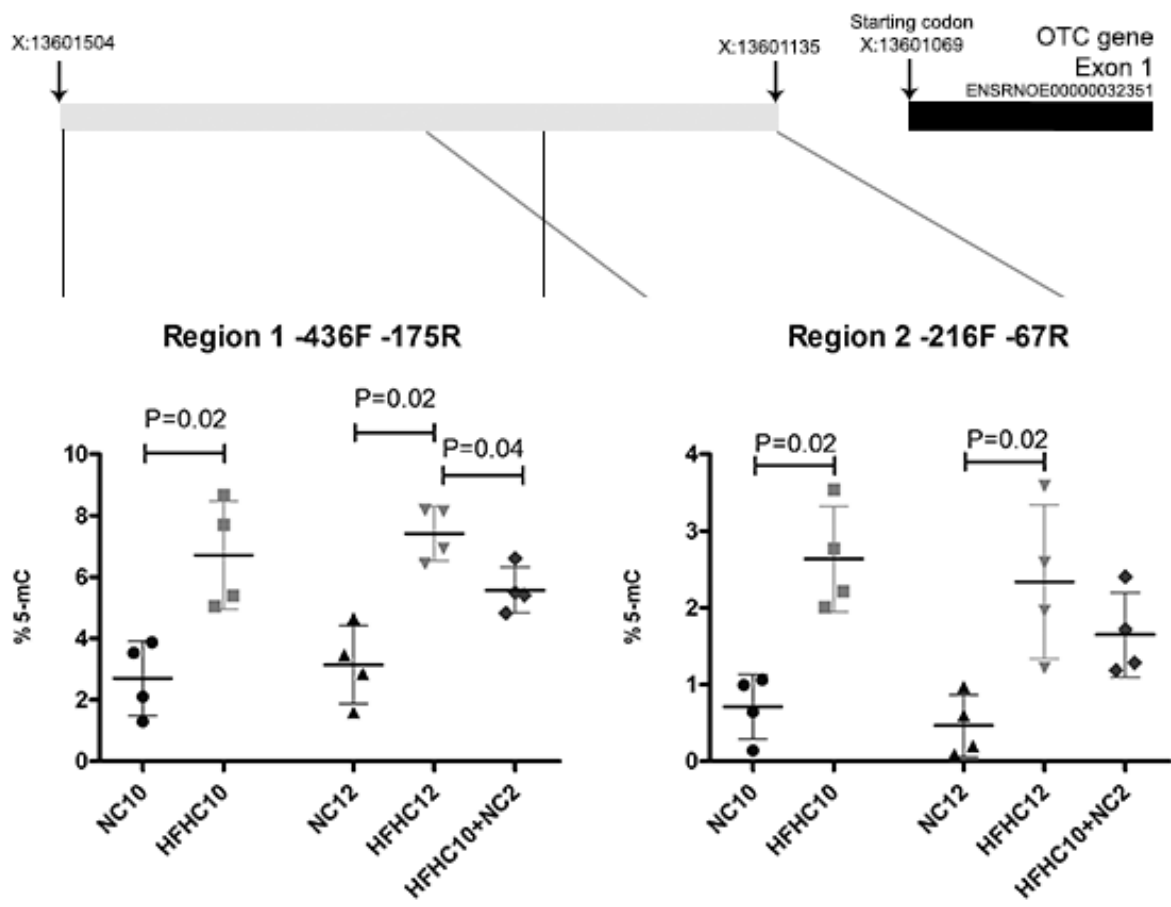


Figure 3



ACCEPTED MANUSCRIPT

Figure 4

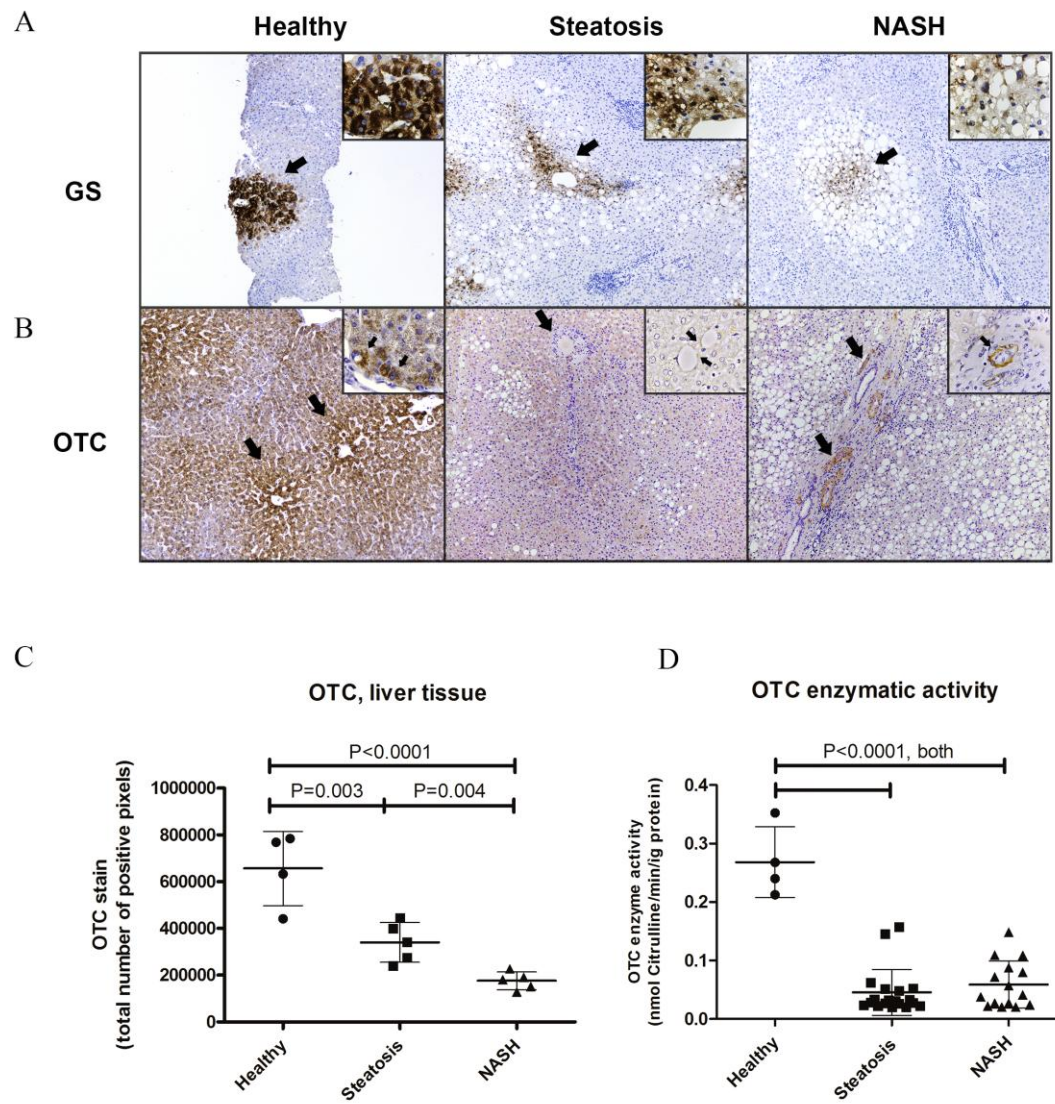


Figure 5

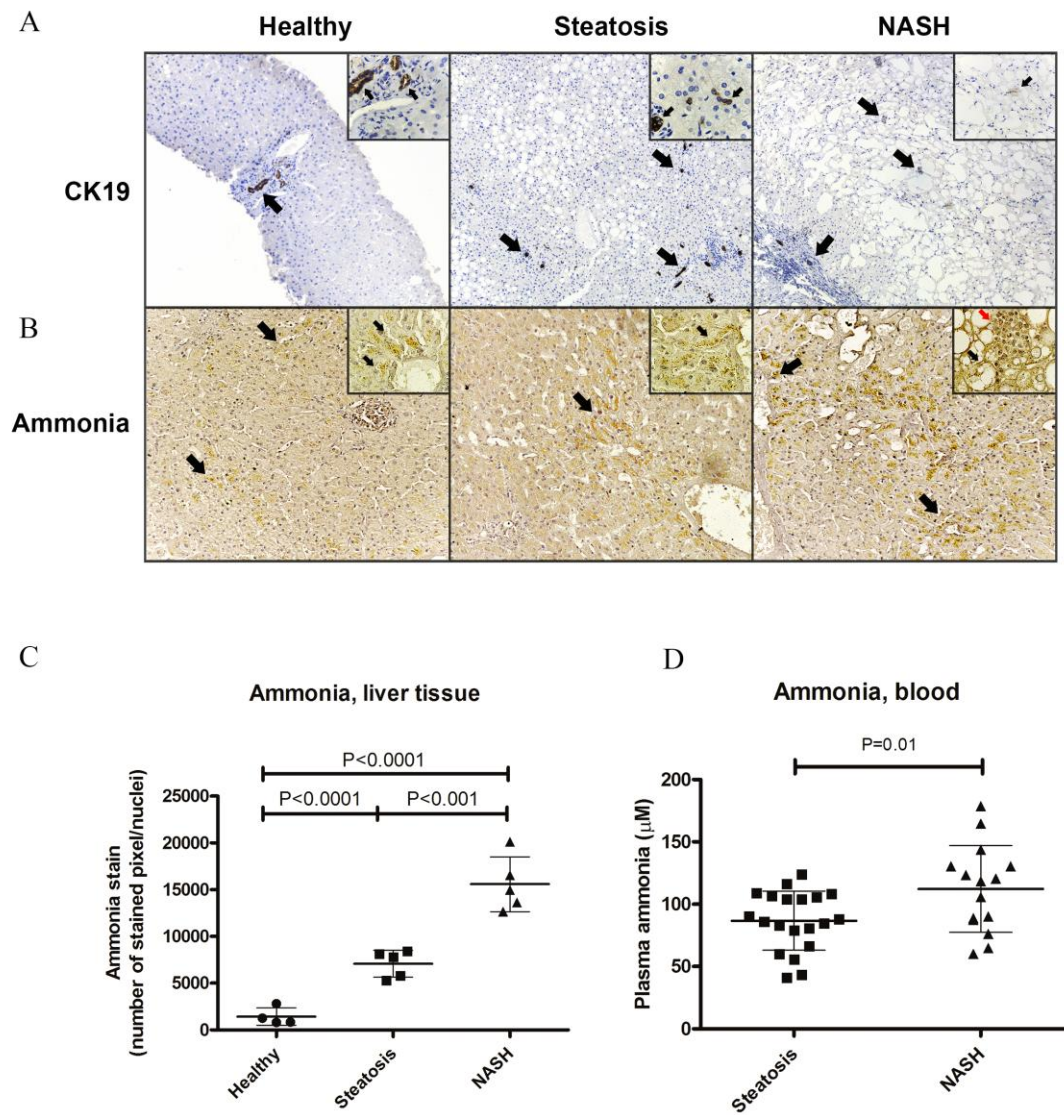
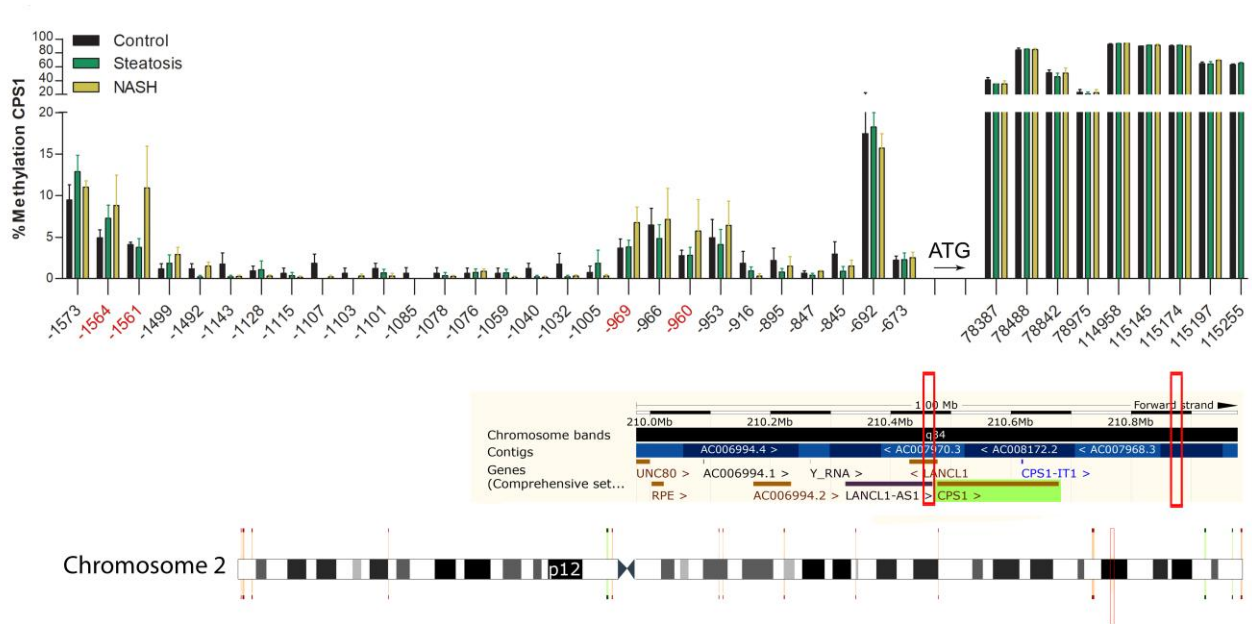
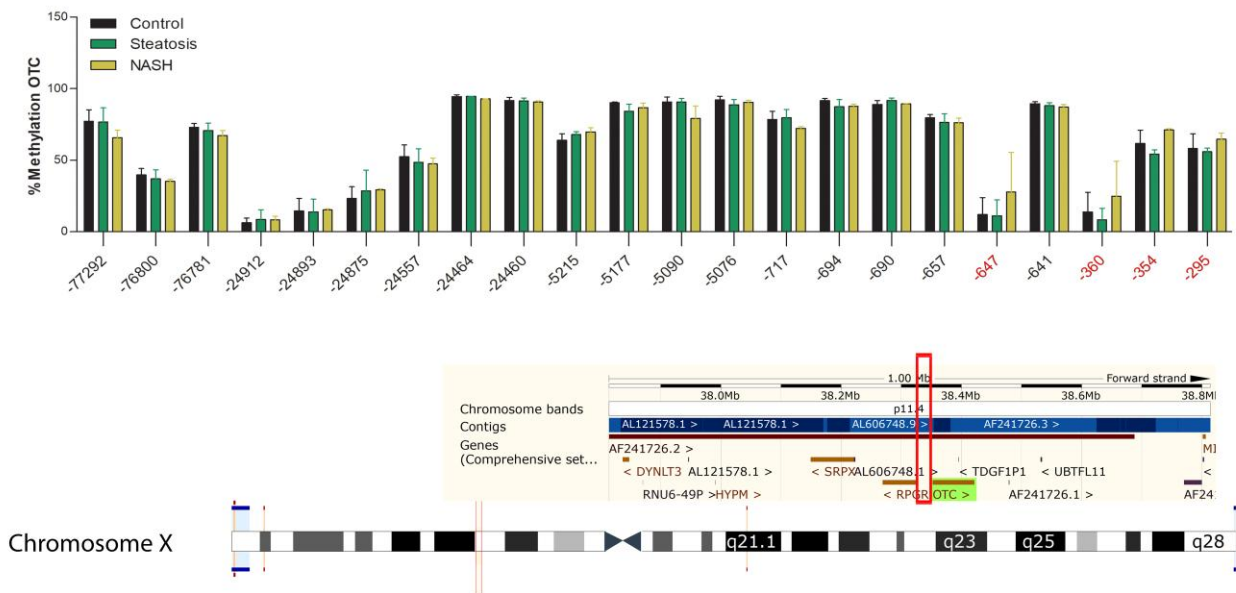


Figure 6

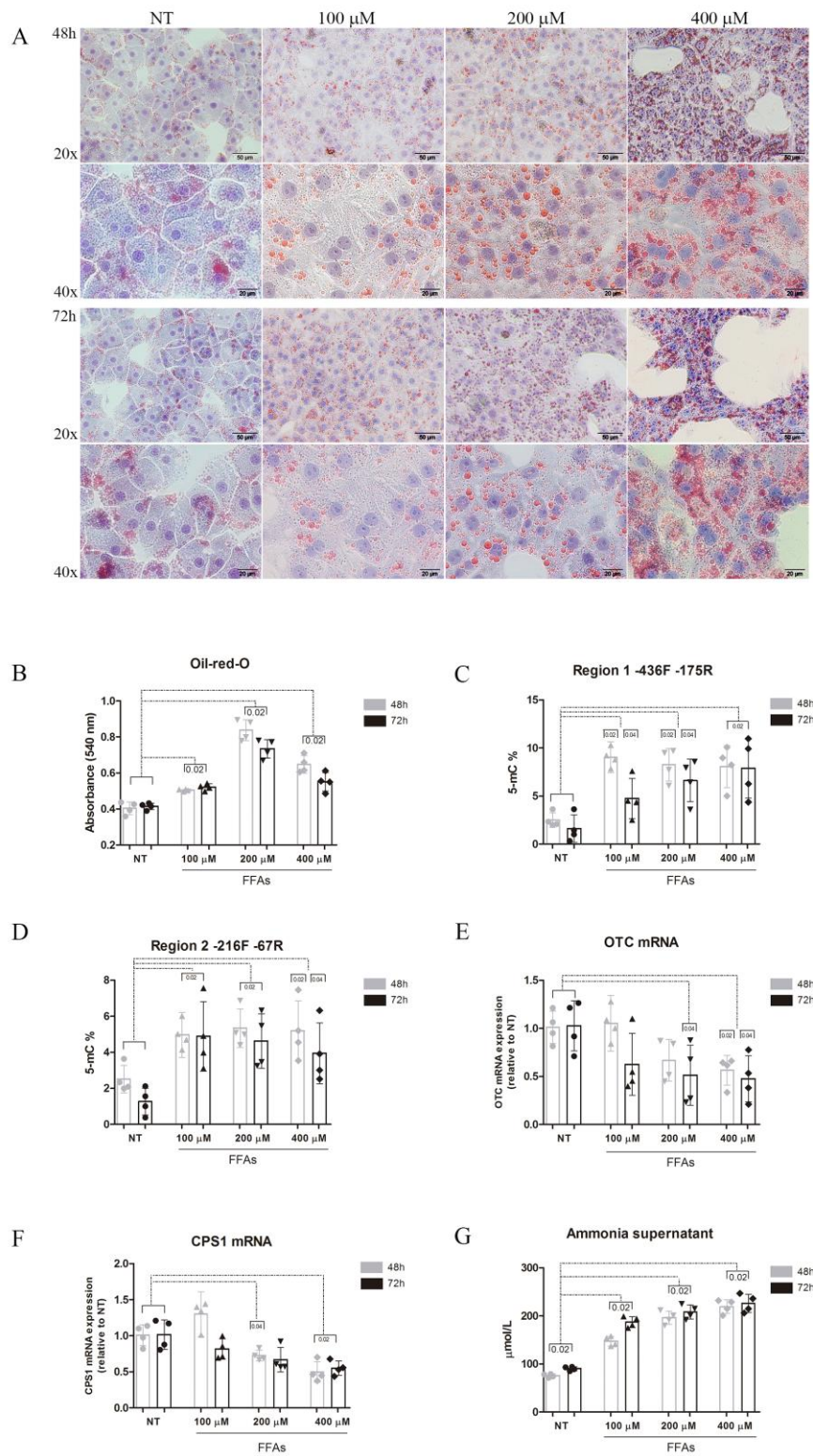


B



ACCEPTED MANUSCRIPT

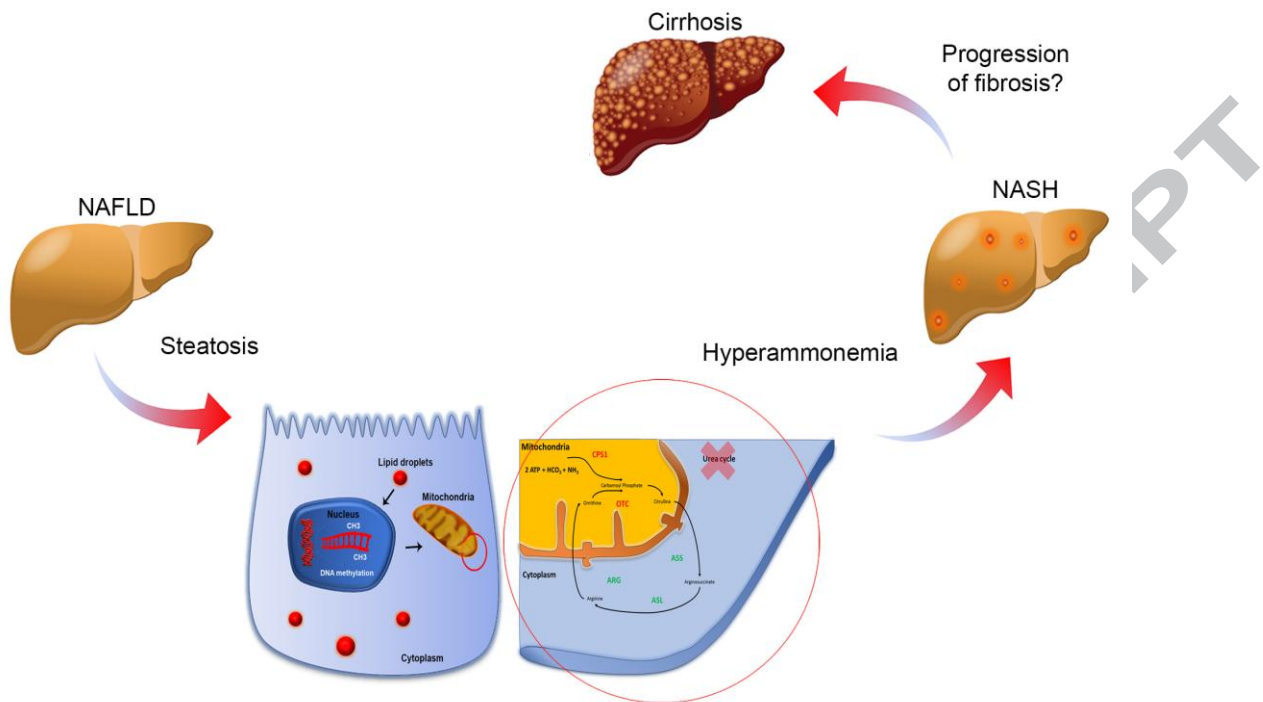
Figure 7



ACCEPTED MANUSCRIPT

Highlights

- Experimental and human NASH is associated with reduced urea cycle enzyme expression
- Hypermethylation of urea cycle enzymes is a potential underlying mechanism
- The functional changes of urea synthesis in NASH is associated with hyperammonemia
- Hyperammonemia can cause progression of liver injury and fibrosis
- Ammonia is a potential novel target for prevention of progression of NASH



ACCEPTED MANUSCRIPT